
Hashing Over Predicted Future Frames for Informed Exploration of Deep Reinforcement Learning

Haiyan Yin Sinno Jialin Pan
 Nanyang Technological University, Singapore
 {haiyanyin, sinnopan}@ntu.edu.sg

Abstract

In reinforcement learning (RL) tasks, an efficient exploration mechanism should be able to encourage an agent to take actions that lead to less frequent states which may yield higher accumulative future return. However, both *knowing about the future* and *evaluating the frequentness of states* are non-trivial tasks, especially for deep RL domains, where a state is represented by high-dimensional image frames. In this paper, we propose a novel informed exploration framework for deep RL tasks, where we build the capability for a RL agent to predict over the future transitions and evaluate the frequentness for the *predicted* future frames in a meaningful manner. To this end, we train a deep prediction model to generate future frames given a state-action pair, and a convolutional autoencoder model to generate deep features for conducting hashing over the seen frames. In addition, to utilize the counts derived from the *seen* frames to evaluate the frequentness for the *predicted* frames, we tackle the challenge of making the hash codes for the predicted future frames to match with their corresponding seen frames. In this way, we could derive a reliable metric for evaluating the novelty of the future direction pointed by each action, and hence inform the agent to explore the least frequent one. We use Atari 2600 games as the testing environment and demonstrate that the proposed framework achieves significant performance gain over a state-of-the-art informed exploration approach in most of the domains.

1 Introduction

Reinforcement learning (RL) involves an agent progressively interacting with an initially unknown environment, in order to learn an optimal policy with the objective of maximizing the cumulative rewards collected from the environment [22]. Throughout the learning process, the RL agent alternates between two primal behaviors: *exploration* - to try out novel states that could potentially lead to high future rewards; and *exploitation* - to perform greedily according to the learned knowledge [22]. In the past, exploitation of learned knowledge has been well studied, while how to efficiently explore through the state space is still remained as a critical challenge, especially for deep RL domains.

In deep RL domains, a state is represented by low-level sensory inputs only, such as image pixels [11, 14, 9], which is often high-dimensional or/and continuous. Thus, the state space for deep RL is huge and often intractable for searching. When performing exploration through such a huge state space, most existing deep RL works (e.g., [25, 3, 24, 19, 18]) adopt a simple exploration heuristic, ϵ -greedy strategy, where the RL agent takes a random action with a probability of ϵ , e.g., via uniform sampling for discrete-action domains [22, 11] or corrupting action with i.i.d. Gaussian noise for continuous-action domains [10]. In such a way, the agent explores the state space without conscious, i.e., without incorporating any meaningful knowledge about the environment. Such exploration heuristic turns out to work well in simple problem domains but fails to handle more challenging

domains, such as those with extremely sparse rewards that lead to exponentially increasing state space, and those with a large action space.

Unlike the unconscious exploratory behavior for agents using ϵ -greedy strategy, when human beings are intending to explore an unfamiliar task domain, one often actively applies domain knowledge for the task, accounts for the state space that has been less frequently visited, and intentionally tries out actions that lead to novel states. In this work, we aim to mimic such exploratory behaviors to improve upon the ϵ -greedy strategy with random action selection, and come up with a more efficient *informed* exploration framework for deep RL agents. On one hand, we develop agent’s knowledge on the environment and make it able to predict the future trajectories. On the other hand, we integrate the developed knowledge with hashing techniques over the high-dimensional state space in order to make the agent be able to realistically evaluate the novelty for the *predicted* future trajectories.

Specifically, in our proposed informed exploration framework, first, we train an action-conditional prediction model to predict future frames given a state-action pair. Second, to perform hashing over the high-dimensional state space seen by the agent, we train a deep convolutional autoencoder to generate high-level features for the state and apply locality-sensitive hashing (LSH) [5] on the high-level state features to generate binary codes to represent each state. However, the learned hashing function is counting over the actually *seen* states, while we need to query the counts for the *predicted* future frames to compute their novelty. Hence, we introduce an additional training phase for the autoencoder to match the hash codes for the *predicted* frames with that of their corresponding ground-truth frames (i.e., the actually *seen* frames). In this way, we are able to utilize the environment knowledge and hashing techniques over the high-dimensional states to generate a reliable novelty evaluation metric for the future direction pointed by each action given a state.

2 Related Work

Recently, works on enhancing the exploration behavior of the deep RL agent have demonstrated great potential in improving the performance of various deep RL task domains. In [12], asynchronous training techniques is adopted and multiple agents are created to perform gradient-based learning to update the model parameters separately in the Atari 2600 domain. In [16], an ensemble of Q-functions is trained to reduce the bias for the values being approximated and increases the exploration depth in the Atari 2600 domain. In [6], an exploration strategy based on maximizing the information gain of the agent’s belief about the environment dynamics is adopted for tasks with continuous states and actions. In [1], the KL-divergence between the probability obtained from a learned dynamics model and that of the actual trajectory is used to measure the surprise over the experience. In [3, 23], the novelty of a state is measured based on count-based mechanisms, and reward shaping is performed by adding a reward bonus term on the Q-value which is computed based on the counts. For all those approaches, the exploration strategy is incorporated either in the function approximation or during the optimization process, and the agent still needs to randomly choose action to explore without relying on any knowledge about the model. In this work, we aim to conduct informed exploration, i.e., to utilize the model-based knowledge to derive a deterministic choice of action for the agent to explore.

Exploration with Deep Prediction Models Recent works aiming to incentivize exploration via deep prediction models have shown promising results for deep RL domains. In [21], an autoencoder model is trained jointly with the policy model, and the reconstruction error from the autoencoder is used to determine the rareness of a state. In [17], a pixelCNN is trained jointly with the policy model as a density model for the state. The prediction gain of a state is measured as the difference of the state density given by the pixelCNN after and before observing that state. In both approaches, the novelty of a state is measured by the loss or output of another model, which is not exact statistics. In our work, we use the counts derived from hashing over the state space to reliably infer the novelty of a state. In [15], which is a mostly related work to ours, an action-conditional prediction model is trained to predict the future frame given a state-action pair. Then they compute the gaussian kernel distance between a predicted future frame and a set of history frames, and inform the agent to take the action that leads to the frame which is most dissimilar compared to a window of recent frames. In our work, we use the same action-conditional architecture as in [15] to construct the prediction model. However, we involve a hashing mechanism to count over the state space to determine the novelty of a state based on the counting statistics. We enable the model to query the exact counting

statistics for the *predicted* frames, and compute the novelty for each action direction based on the novelty evaluated on *multi*-step prediction.

Hashing for Deep RL Domain Running RL algorithms on the discretized features yields faster learning and promising performance. It is shown that the latent features learned by autoencoder trained in an unsupervised manner is of great promise to efficiently discretize the high-dimensional state space [4]. In [23], the state space for Atari 2600 domain is first discretized using the latent features derived from an autoencoder model. Then hashing is performed to encourage exploration by computing a reward bonus term in a form like MBIE-EB [20]. Our work also introduce hashing over the state space based on latent features trained from deep autoencoder model, but the exploration mechanism is significantly different from [23]. First, in our work, we count over the actually *seen* image frames, but query the hash for the *predicted* frames. Second, as the reward bonus is added to the function approximation target in their approach, the counts for future states influence their previous states backwards via bellman equation, whereas in our work, the count is used for informed exploration, which does not have direct influence on the approximated Q-values.

3 Methodology

3.1 Notations

In this paper, we consider a discounted finite-horizon Markov Decision Process (MDP) with discrete actions. Formally, it is defined by a tuple $(\mathcal{S}, \mathcal{A}, \mathcal{P}, \mathcal{R}, \gamma)$, where \mathcal{S} is a set of states which could be high-dimensional or continuous, \mathcal{A} is a set of actions, \mathcal{P} is a state transition probability distribution with $\mathcal{P}(s'|s, a)$ specifying the probability for transiting to state s' after issuing action a at state s , \mathcal{R} is a reward function mapping each state-action pair to a reward in \mathbb{R} , and $\gamma \in [0, 1]$ is a discount factor. The goal of the RL agent is to learn a policy π that maximizes the expected cumulative future rewards given the policy: $\mathbb{E}_\pi[\sum_{t=0}^T \gamma^t \mathcal{R}(s_t, a_t)]$. In the context of deep RL, at each step t , a RL agent receives a state observation $\mathcal{S}_t \in \mathbb{R}^{r \times m \times n}$, where r is the number of consequent frames to represent a state, and $m \times n$ is the dimension for each frame. The agent selects an action $a_t \in \mathcal{A}$ among all the l possible choices, and receives a reward $r_t \in \mathbb{R}$.

3.2 Informed Exploration Framework

We propose an informed exploration framework to mimic the exploratory behavior of human beings under an unfamiliar task domain. Generally, the RL agent no longer randomly selects an action to explore without incorporating any domain knowledge. Instead, we aim to let the agent intentionally select the action that leads to the least frequent future states and thus explore the state space in an informed and deterministic manner. To this end, we build the capability of the RL agent on performing the following two tasks: 1) predicting over future transitions, and 2) evaluating the visiting frequency for those predicted *future* frames.

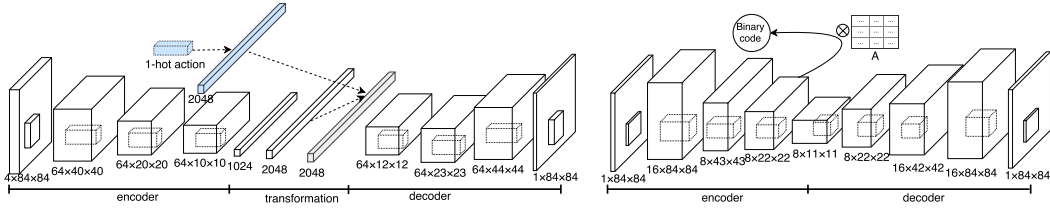


Figure 1: Deep neural network architectures adopted for informed exploration. **Left:** action-conditional prediction model for predicting over future transition frames; **right:** autoencoder model for conducting hashing over the state space.

3.2.1 Learning Transition Model with Prediction Network

The architecture for action-conditional prediction is shown in Figure 1 (left). To be specific, we train a deep prediction model $f : (\mathcal{S}_t, a_t) \rightarrow \mathcal{S}_{t+1}$ to make the agent able to predict over the future

transitions given a state-action pair. The state input \mathcal{S}_t is a set of r recent image frames, and the action input a_t is represented by $\mathbf{a}_t \in \mathbb{R}^l$, which is a one-hot vector, where l is the number of actions for the task domain. To predict a new state, the model predicts one single frame at a time, denoted as $\bar{\mathbf{s}} \in \mathbb{R}^{m \times n}$. The new state \mathcal{S}_{t+1} is formed by concatenating the predicted new frame with the most recent $r-1$ frames. We adopt the action-conditional transformation as proposed in [15] to form a joint feature for the state input and the action input. Specifically, the state input is first passed through three stacked convolutional layers to form a feature vector $\mathbf{h}_t^s \in \mathbb{R}^h$. Then the state feature \mathbf{h}_t^s and the one-hot action feature \mathbf{a}_t perform a linear transformation by multiplying with their corresponding transformation matrix $\mathbf{W}_t^s \in \mathbb{R}^{k \times h}$ and $\mathbf{W}_t^a \in \mathbb{R}^{k \times l}$. After the linear transformation, both features are shaped with the same dimensionality. Then the features for the state and action after the linear transformation performs a multiplicative interaction to form a joint feature as follows,

$$\mathbf{h}_t = \mathbf{W}_t^s \mathbf{h}_t^s \odot \mathbf{W}_t^a \mathbf{a}_t.$$

Afterwards, the joint feature \mathbf{h}_t is passed through stacked deconvolutional layers and a sigmoid layer to form the final prediction output. To predict over multiple future steps, the prediction model progressively composes the new state using its prediction result to predict the next-step transition.

3.2.2 Hashing over the State Space with Autoencoder and LSH

To evaluate the novelty of a state, we adopt a hashing model to count over the state space. We first train an autoencoder model on frames, $g: \mathbf{s} \in \mathbb{R}^{m \times n} \rightarrow \hat{\mathbf{s}} \in \mathbb{R}^{m \times n}$, in an unsupervised manner with the reconstruction loss as follows [8],

$$\mathcal{L}_{\text{rec}}(\mathbf{s}_t) = -\frac{1}{mn} \sum_{j=1}^n \sum_{i=1}^m (\log p(\hat{\mathbf{s}}_{t_{ij}})), \quad (1)$$

where $\hat{\mathbf{s}}_{t_{ij}}$ is the reconstructed pixel at the i -th row and the j -th column. The architecture for the autoencoder model is shown in Figure 1 (right). To be specific, each convolutional layer is followed by a Rectifier Linear Unit (ReLU) [13] layer and a max pooling layer with a kernel size 2×2 . To discretize the state space, we hash over the last frame s_t of each state. We adopt the output of the last ReLU layer from the encoder as the high-level state features, and denote by $\phi(\cdot)$ the corresponding feature map that generates the high-level feature vector $\mathbf{z}_t \in \mathbb{R}^d$ of a state, i.e., $\phi(\mathbf{s}_t) = \mathbf{z}_t$. To further discretize the state feature, locality-sensitive hashing (LSH) [5] is adopted upon \mathbf{z}_t . To this end, a projection matrix $\mathbf{A} \in \mathbb{R}^{p \times d}$ is randomly initialized with i.i.d. entries drawn from a standard Gaussian $\mathcal{N}(0, 1)$. Then by projecting feature \mathbf{z} through \mathbf{A} , the sign of the outputs form a binary code, $\mathbf{c} \in \mathbb{R}^p$. With the introduced discretization scheme, we are able to count over the state space for the problem domain. During the RL process, a hash table \mathcal{H} is created. The count for a state \mathcal{S}_t , denoted by ψ_t , can be stored, queried and updated from the hash table. Overall, the process for counting over a state \mathcal{S}_t is expressed in the following formulas.

$$\mathbf{z}_t = \phi(\mathbf{s}_t), \quad \mathbf{c}_t = \text{sgn}(\mathbf{A}\mathbf{z}_t), \quad \text{and} \quad \psi_t = \mathcal{H}(\mathbf{c}_t). \quad (2)$$

3.2.3 Matching the Prediction with Reality

To derive the novelty for the *predicted* frames while updating the hash table with *seen* frames, we need to match the predictions with realities, i.e., make the hash codes for the *predicted* frames to be the same as their corresponding ground-truth *seen* frames in training. To this end, we introduce an additional training phase for the autoencoder model $g(\cdot)$. To make the hash codes to be the same, the derived feature vectors of the predicted frames and the ground-truth seen frames through $\phi(\cdot)$ need to be close to each other. We introduce an additional loss function of a pair of a ground-truth seen frame and a predicted frame $(\mathbf{s}_t, \bar{\mathbf{s}}_t)$ as follows,

$$\mathcal{L}_{\text{mat}}(\mathbf{s}_t, \bar{\mathbf{s}}_t) = \|\phi(\mathbf{s}_t) - \phi(\bar{\mathbf{s}}_t)\|_2 \quad (3)$$

Finally, by combining (1) and (3), we define the following overall loss function,

$$\mathcal{L}(\mathbf{s}_t, \bar{\mathbf{s}}_t; \theta) = \mathcal{L}_{\text{rec}}(\mathbf{s}_t) + \mathcal{L}_{\text{rec}}(\bar{\mathbf{s}}_t) + \lambda \mathcal{L}_{\text{mat}}(\mathbf{s}_t, \bar{\mathbf{s}}_t), \quad (4)$$

where θ is the parameter for the autoencoder.

Note that even though the prediction model could generate almost identical frames, training the autoencoder with only the reconstruction loss may lead to distinct state codes in all the task domains

(details will be shown in Section 4). Therefore, the effort for matching the codes is necessary. However, matching the state code while guaranteeing a satisfying reconstruction behavior is extremely challenging. Fine tuning an autoencoder fully trained with \mathcal{L}_{rec} by the code matching loss \mathcal{L}_{mat} would fast disrupt the reconstruction behavior before the code loss could decrease to the expected level. Training the autoencoder from scratch with both \mathcal{L}_{rec} and \mathcal{L}_{mat} is also difficult, as \mathcal{L}_{mat} is initially very low and \mathcal{L}_{rec} is very high. The network can hardly find a direction to consistently decrease \mathcal{L}_{rec} with such an imbalance. Therefore, in this work, we propose to train the autoencoder for two phases, where the first phase uses \mathcal{L}_{rec} to train until convergence, and the second phase uses the composed loss function \mathcal{L} as proposed in (4) to address the requirement for matching the prediction with reality.

3.2.4 Computing Novelty for States

Once the prediction model $f(\cdot)$ and the autoencoder model $g(\cdot)$ are both trained, the agent could perform informed exploration in the following manner. At each step, the agent performs exploration with a probability less than ϵ and perform greedy action selection otherwise. Given the state S_t , when performing exploration, the agent predicts through the future trajectories with length r for all the possible actions $a_j \in \mathcal{A}$. Formally, the novelty score for an action a_j given state S_t , denoted by $\rho(a_j|S_t)$, is computed as

$$\rho(a_j|S_t) = \sum_{i=1}^q \frac{\beta^{i-1}}{\sqrt{\psi_{t+i} + 0.01}}, \quad (5)$$

where ψ_{t+i} is the count for the future state S_{t+i} derived from (2) for the predicted frames $\{\bar{s}_{t+j}\}_{j=1}^i$, q is the predefined prediction length, and β is a real-valued discount rate. After evaluating the novelty for all the possible actions, the agent selects the one with the highest novelty score to explore. Overall, the policy for the RL agent with the proposed informed exploration strategy is defined as:

$$a_t = \begin{cases} \arg \min_a [\mathcal{Q}(S_t, a)] & p \geq \epsilon \\ \arg \max_a [\rho(a|S_t)] & p < \epsilon \end{cases}$$

where $\mathcal{Q}(S_t, a)$ is the Q-value function, and p is a random value sampled from Uniform (0,1).

4 Experiments

In the empirical evaluation, we use the Arcade Learning Environment (ALE) [2], which consists of Atari 2600 video games as the testing domain. We choose 5 representative games that require significant exploration to learn the policy: *Breakout*, *Freeway*, *Frostbite*, *Ms-Pacman* and *Q-bert*. Among the five games, *Frostbite* has a large action space that consists of a full set of 18 actions, *Breakout* has a state distribution that changes significantly as the ability of the policy network changes, and all the others have sparse rewards. For all the tasks, we use the state representation that concatenates 4 consequent image frames of size 84×84 .

4.1 Evaluation on Prediction Model

The architecture of the prediction model is identical to the one shown in Figure 1 (left). To train the prediction model, we create a training dataset which consists of 500,000 transition records generated by a fully trained DQN agent performing under ϵ -greedy with uniform random action selection, where ϵ is set equal to 0.3. During training, we adopt Adam [7] as the optimization algorithm and use a learning rate of 10^{-3} and a mini-batch size of 100. Moreover, we discount the gradient scale by multiplying the gradient value by 10^{-2} . The state input is normalized by dividing the pixel values by 255.

We show the pixel prediction loss in mean square error (MSE) for multi-step future prediction in Table 1. For all the task domains, the prediction errors are within a small scale. The prediction error increases with the increase of the prediction length. We demonstrate that the trained prediction models are able to generate realistic future frames which are visualized to be very close to the ground-truth frames from the results shown in Figure 2.

Game	1-step	3-step	5-step	10-step
Breakout	1.114e-05	3.611e-04	4.471e-04	5.296e-04
Freeway	2.856e-05	0.939e-05	1.424e-04	2.479e-04
Frostbite	7.230e-05	2.401e-04	5.142e-04	1.800e-03
Ms-Pacman	1.413e-04	4.353e-04	6.913e-04	1.226e-03
Q-bert	5.300e-05	1.570e-04	2.688e-04	4.552e-04

Table 1: The prediction loss in MSE for the trained prediction models.

4.2 Evaluation on Hashing with Autoencoder and LSH

The architecture for the autoencoder model is identical to that shown in Figure 1 (right). The autoencoder is trained on a dataset collected in an identical manner as that for the prediction model. It is trained under two phases. In the first phase, it is trained with only reconstruction loss. We use Adam as optimization algorithm, 10^{-3} as learning rate, a mini-batch size of 100 and discount the gradient by multiplying 10^{-2} . In the second phase, we train the autoencoder based on the loss in (4). In the second phase, we use Adam as optimization algorithm, 10^{-4} as learning rate, a mini-batch size of 100, and λ value of 0.01. We discount the gradient by multiplying the gradient value by 5×10^{-3} .

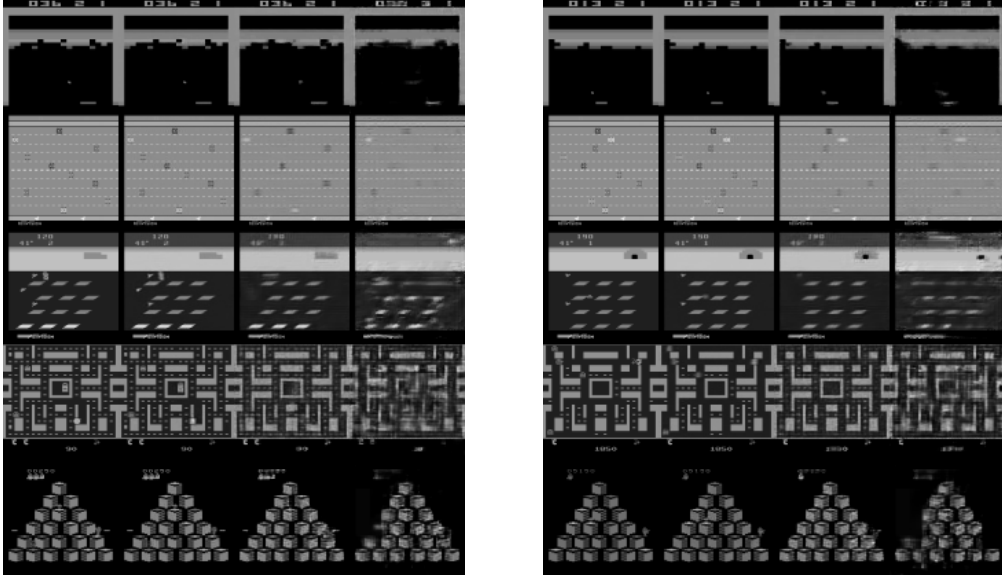
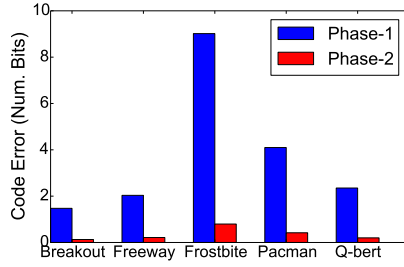
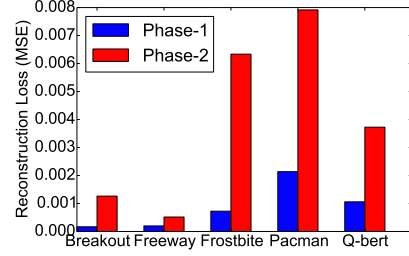


Figure 2: The prediction and reconstruction result for each task domain. For each task, we present 2 sets of frames, where each set consists of four frames. The 2 sets of frames for each domain are put side-by-side in a row. The four frames for each set are organized as follows: (1) the **ground-truth** frame seen by the agent; (2) the **predicted** frame by the prediction model; (3) the **reconstruction** of autoencoder trained only with reconstruction loss; (4) the **reconstruction** of autoencoder trained after the second phase (i.e., trained with both reconstruction loss and code matching loss).

Overall, it is extremely challenging to match the state codes for the *predicted* frames and their corresponding *seen* frames while maintaining a satisfying reconstruction performance. We demonstrate this in Figure 3 (a) by showing the *code loss*, which is measured in terms of the number of mismatch in binary codes between a pair of predicted frame and its corresponding ground-truth frame. The presented result is derived by averaging over 10,000 pairs of codes. First, the result shows that without the second phase, it is impossible to perform hashing with autoencoder trained only by the reconstruction loss, since the average *code losses* are above 1 in all the domains and with distinct hash codes, the count values returned from querying the hash table are meaningless. Second, the result shows that after the training of the second phase, the *code loss* is significantly reduced.



(a) Code Loss



(b) Reconstruction Loss

Figure 3: Comparison of the code loss and reconstruction loss (MSE) for the autoencoder model after the training of phase 1 and phase 2.

We also show the reconstruction errors measured in terms of MSE after the training of the two phases for each domain in Figure 3 (b). By incorporating the code matching loss, the reconstruction behavior for the autoencoder receives slightly negative effect. A comparison of frame reconstruction effect after the training of the two phases are shown in Figure 2. It is shown that after training to match the state codes, the reconstructed frames are slightly blurred, but still able to reflect the essential features in each problem domain except for *Q-bert*.

Moreover, we use *Breakout* as an illustrative example to demonstrate that the presented hashing framework can generate meaningful hash codes for *predicted* future frames (Figure 4). For a given ground-truth frame, we show the predicted frames with length 5 for taking each action. It can be found that the trajectories of ball positions are predicted to be the same regardless of the action choice, and different actions lead to different board positions. For the hash codes, as the first two actions, *no-op* and *fire*, lead to little change in frames, almost all the future frames are hashed into the same code. The last two actions, *right* and *left*, lead to significant changes in board position, so the codes for future frames are much more distinct from each other. The result also shows that the hash code is less sensitive to ball position compared to the board position in this game domain.

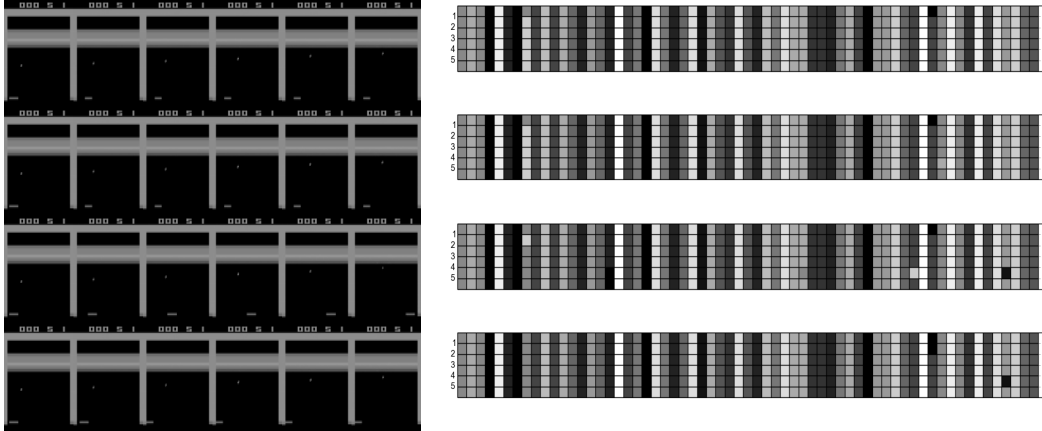


Figure 4: **Left:** the predicted future trajectories for each action in *Breakout*. In each row, the first frame is the *ground-truth* frame and the following five frames are the *predicted* future trajectories with length 5. In each row, the agent takes one of the following actions (constantly): (1) no-op; (2) fire; (3) right; (4) left. **Right:** the hash codes for the frames in the same row ordered in a top-down manner. To save the space, four binary codes are grouped into one hex code, i.e., in a range of 0 to 15, and the color map is normalized linearly by the hex value.

4.3 Evaluation on Informed Exploration Framework

To evaluate the efficiency of the proposed informed exploration framework, we integrate it into the DQN algorithm [11]. We compare it with two baselines: (1) DQN that performs ϵ -greedy with uniform random choice of action for exploration, denoted by DQN-Random; (2) the state-of-the-art informed exploration approach proposed in [15], denoted by DQN-Informed. The proposed informed exploration approach in this paper is denoted by DQN-Informed-Hash. Note that both DQN-Informed and the proposed approach adopt DQN as the base algorithm. We run the experiment by following the standard setting used in [11]. For all the methods, we train the agent over 50 million frames and evaluate the RL agent over 100 episodes of game play. We use $q = 3$ as the length for hashing over future frames. We report the result in Table 2.

Model	Breakout	Freeway	Frostbite	Ms-Pacman	Q-bert
DQN-Random	401.2 (26.9) ¹	30.9 (0.2)	328.3 (250.5) ¹	2281 (53)	3876 (106)
DQN-Informed	0.93 (1.8) ²	32.2 (0.2)	1287.01 (314.3) ²	2522 (57)	8238 (498)
DQN-Informed-Hash	451.93 (45.79)	33.92 (0.14)	1812.10 (433.64)	3526.60 (398.62)	8827.83 (531.64)

¹ Scores are obtained from [11].

² Scores are obtained by implementing DQN-Informed by us in tasks not used in [15].

Table 2: Performance score for the proposed approach and baseline RL approaches.

The performance scores for DQN-Random and DQN-Informed are obtained from [15] except for game *Breakout* and *Frostbite*, which are not included in their work. Among all the test domains, DQN-Informed-Hash outperforms the baseline approaches, and there are significant performance gains observed in each domain. Note that in *Breakout*, the agent fails to progress with DQN-Informed and always scores almost 0. It may due to that the kernel-based pixel distance evaluation metric used in DQN-Informed encourages the agent to explore states that is dissimilar from the recent history, which is insufficient to let the agent explore. Note that DQN-Informed-Hash demonstrates the superior performance with a *deterministic* exploration mechanism. It indicates that counting over the predicted future frames could provide a meaningful direction for exploration.

5 Conclusion

In this paper, we propose an informed exploration framework for deep RL tasks with discrete action space. By incorporating a deep convolutional prediction model over future transitions and a hashing mechanism based on a deep autoencoder model and LSH, we enable the agent to predict over the future trajectories and intuitively evaluate the novelty for each future action direction based on the hashing result. The empirical result on Atari 2600 domain shows that the proposed informed exploration framework could efficiently encourage exploration in several challenging deep RL domains.

References

- [1] Joshua Achiam and Shankar Sastry. Surprise-based intrinsic motivation for deep reinforcement learning. 2017.
- [2] M. G. Bellemare, Y. Naddaf, J. Veness, and M. Bowling. The arcade learning environment: An evaluation platform for general agents. *Journal of Artificial Intelligence Research*, 47:253–279, jun 2013.
- [3] Marc Bellemare, Sriram Srinivasan, Georg Ostrovski, Tom Schaul, David Saxton, and Remi Munos. Unifying count-based exploration and intrinsic motivation. In *Advances in Neural Information Processing Systems*, pages 1471–1479, 2016.
- [4] Charles Blundell, Benigno Uria, Alexander Pritzel, Yazhe Li, Avraham Ruderman, Joel Z Leibo, Jack Rae, Daan Wierstra, and Demis Hassabis. Model-free episodic control. *arXiv preprint arXiv:1606.04460*, 2016.
- [5] Moses S Charikar. Similarity estimation techniques from rounding algorithms. In *Proceedings of the thirty-fourth annual ACM symposium on Theory of computing*, pages 380–388. ACM, 2002.
- [6] Rein Houthoofd, Xi Chen, Yan Duan, John Schulman, Filip De Turck, and Pieter Abbeel. Vime: Variational information maximizing exploration. In *Advances in Neural Information Processing Systems*, pages 1109–1117, 2016.
- [7] Diederik P. Kingma and Jimmy Ba. Adam: A method for stochastic optimization. *CoRR*, abs/1412.6980, 2014.

- [8] Diederik P Kingma and Max Welling. Auto-encoding variational bayes. *arXiv preprint arXiv:1312.6114*, 2013.
- [9] Sergey Levine, Chelsea Finn, Trevor Darrell, and Pieter Abbeel. End-to-end training of deep visuomotor policies. *JMLR*, 17(39):1–40, 2016.
- [10] Timothy P Lillicrap, Jonathan J Hunt, Alexander Pritzel, Nicolas Heess, Tom Erez, Yuval Tassa, David Silver, and Daan Wierstra. Continuous control with deep reinforcement learning. *arXiv preprint arXiv:1509.02971*, 2015.
- [11] V. Mnih, K. Kavukcuoglu, D. Silver, A. a Rusu, J. Veness, M. G. Bellemare, A. Graves, M. Riedmiller, A. K. Fidjeland, G. Ostrovski, S. Petersen, A. Sadik C. Beattie, I. Antonoglou, D. Kumaran H. King, D. Wierstra, S. Legg, and D. Hassabis. Human-level control through deep reinforcement learning. *Nature*, 2015.
- [12] Volodymyr Mnih, Adria Puigdomenech Badia, Mehdi Mirza, Alex Graves, Timothy P Lillicrap, Tim Harley, David Silver, and Koray Kavukcuoglu. Asynchronous methods for deep reinforcement learning. In *International Conference on Machine Learning*, 2016.
- [13] Vinod Nair and Geoffrey E Hinton. Rectified linear units improve restricted boltzmann machines. In *Proceedings of the 27th international conference on machine learning (ICML-10)*, pages 807–814, 2010.
- [14] Junhyuk Oh, Valliappa Chockalingam, Satinder Singh, and Honglak Lee. Control of memory, active perception, and action in minecraft. *ICML*, 2016.
- [15] Junhyuk Oh, Xiaoxiao Guo, Honglak Lee, Richard L Lewis, and Satinder Singh. Action-conditional video prediction using deep networks in atari games. In *Advances in Neural Information Processing Systems 28*, pages 2845–2853. Curran Associates, Inc., 2015.
- [16] Ian Osband, Charles Blundell, Alexander Pritzel, and Benjamin Van Roy. Deep exploration via bootstrapped dqn. In *Advances In Neural Information Processing Systems*, pages 4026–4034, 2016.
- [17] Georg Ostrovski, Marc G Bellemare, Aaron van den Oord, and Remi Munos. Count-based exploration with neural density models. *arXiv preprint arXiv:1703.01310*, 2017.
- [18] Emilio Parisotto, Jimmy Ba, and Ruslan Salakhutdinov. Actor-mimic deep multitask and transfer reinforcement learning. In *ICLR*, 2016.
- [19] Tom Schaul, John Quan, Ioannis Antonoglou, and David Silver. Prioritized experience replay. In *ICLR*, 2016.
- [20] Satinder P Singh, Andrew G Barto, and Nuttapon Chentanez. Intrinsically motivated reinforcement learning. In *NIPS*, volume 17, pages 1281–1288, 2004.
- [21] Bradley C Stadie, Sergey Levine, and Pieter Abbeel. Incentivizing exploration in reinforcement learning with deep predictive models. *arXiv preprint arXiv:1507.00814*, 2015.
- [22] Richard S Sutton and Andrew G Barto. *Reinforcement learning: An introduction*, volume 1. MIT press Cambridge, 1998.
- [23] Haoran Tang, Rein Houthooft, Davis Foote, Adam Stooke, Xi Chen, Yan Duan, John Schulman, Filip De Turck, and Pieter Abbeel. # exploration: A study of count-based exploration for deep reinforcement learning. *arXiv preprint arXiv:1611.04717*, 2016.
- [24] Hado Van Hasselt, Arthur Guez, and David Silver. Deep reinforcement learning with double q-learning. In *AAAI*, pages 2094–2100, 2016.
- [25] Ziyu Wang, Tom Schaul, Matteo Hessel, Hado van Hasselt, Marc Lanctot, and Nando de Freitas. Dueling network architectures for deep reinforcement learning. In *ICML*, pages 1995–2003, 2016.

Appendix A.

Informed Exploration Algorithm

Algorithm 1: Informed exploration via hashing over predicted future frames.

```

1 Train the prediction model  $f: \mathcal{S}^{r \times m \times n}, a^l \rightarrow \bar{s}^{m \times n}$ , the autoencoder model  $g: \mathcal{S}^{m \times n} \rightarrow \hat{s}^{m \times n}$ .
2 Initialize  $\mathcal{A}^{p \times d}$  with i.i.d. entries drawn from standard Gaussian  $\mathcal{N}(0, 1)$ .
3 Initialize an empty hash table  $\mathcal{H}(\cdot) \equiv 0$ , and a Q-function  $\mathcal{Q}: \mathcal{S}^{r \times m \times n} \rightarrow q^l$ 
4 for each episode do
5   while not terminal do
6     Receive a state observation  $\mathcal{S}_t$  from the environment.
7     Compute the value  $\epsilon_t$ .
8     Draw  $r \sim \text{Uniform}(0, 1)$ 
9     if  $r < \epsilon_t$  then
10      ▷ Informed exploration.
11      for  $k=1, \dots, l$  do
12        Let novelty  $\rho(a_k | \mathcal{S}_t) = 0$ .
13        Let  $a_t = a_k$ .
14        for  $i = 0 \rightarrow q-1$  do
15          Predict  $\bar{s}_{t+i+1} = f(\mathcal{S}_{t+i}, a_{t+i})$ .
16          Compute latent feature  $z_{t+i+1} = \phi(\bar{s}_{t+i+1})$ .
17          Compute hash code  $c_{t+i+1} = \text{sgn}(\mathcal{A} \cdot z_{t+i+1})$ .
18          Derive the count  $\psi_{t+i+1} = \mathcal{H}(c_{t+i+1})$ .
19          Update novelty  $\rho(a_k | \mathcal{S}_t)$  based on  $\psi_{t+i+1}$ .
20          Update  $\mathcal{S}_{t+i+1}[1:r-1, :, :] = \mathcal{S}_{t+i}[2:r, :, :]$ ,  $\mathcal{S}_{t+i+1}[r, :, :] = \bar{s}_{t+i+1}$ 
21          Let  $a_{t+i+1} = \text{argmax}_a \mathcal{Q}(\mathcal{S}_{t+i+1})$ .
22        end
23      end
24      Let  $a_t = \text{argmax}_a \rho(a | \mathcal{S}_t)$ . ▷ Deterministically explore the least frequent action.
25    else
26      Let  $a_t = \text{argmax}_a \mathcal{Q}(\mathcal{S}_t)$  ▷ Greedy.
27    end
28    Take action  $a_t$ , and observe reward  $r_t$ .
29    Compute hash code for observed state  $c_t = \text{sgn}(\mathcal{A} \cdot \phi(s_t))$  ▷ Hashing.
30    Update hash table  $\mathcal{H}(c_t) \leftarrow \mathcal{H}(c_t) + 1$ 
31    Update Q-function on sampled transitions frequently. ▷ Q-learning.
32  end
33 end

```

Appendix B.

Result for Multi-step Prediction over Future Frames

In this section, we show the multi-step prediction result over future frames in each task domain. We demonstrate the predicted future frames with a prediction length of 6. For each task, we illustrate 2 sets of prediction results, where each set consists of 2 rows. The first frame from the first row corresponds to the *ground-truth* frame s_t , and the following 6 frames in the first row correspond to the *ground-truth* frames from s_{t+1} to s_{t+6} . The frames in the second row correspond to the *predicted* future frames from \bar{s}_{t+1} to \bar{s}_{t+6} .

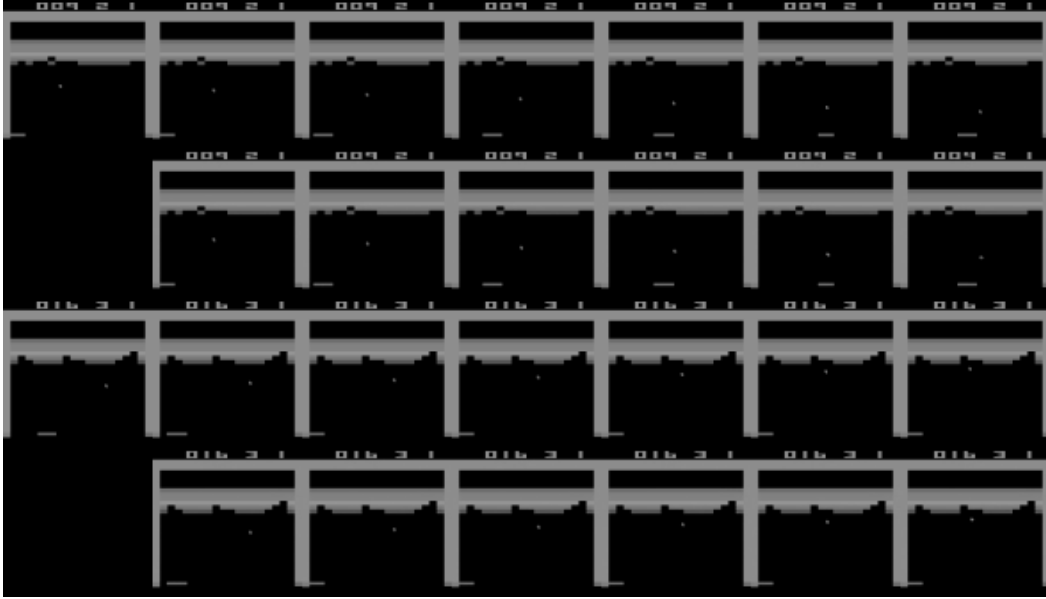


Figure 5: Multi-step prediction result for *Breakout*.

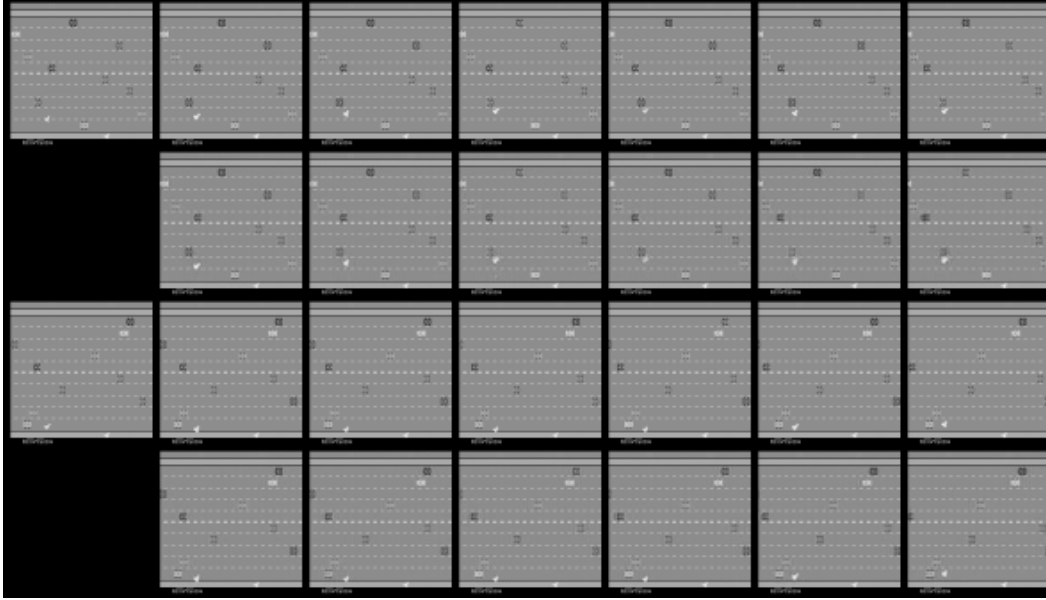


Figure 6: Multi-step prediction result for *Freeway*.

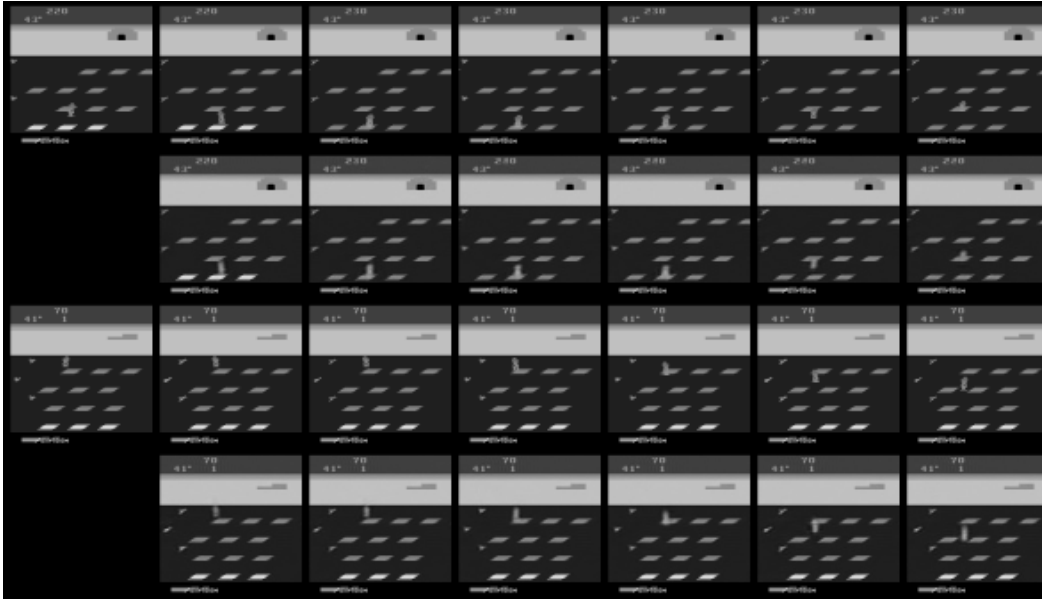


Figure 7: Multi-step prediction result for *Frostbite*.

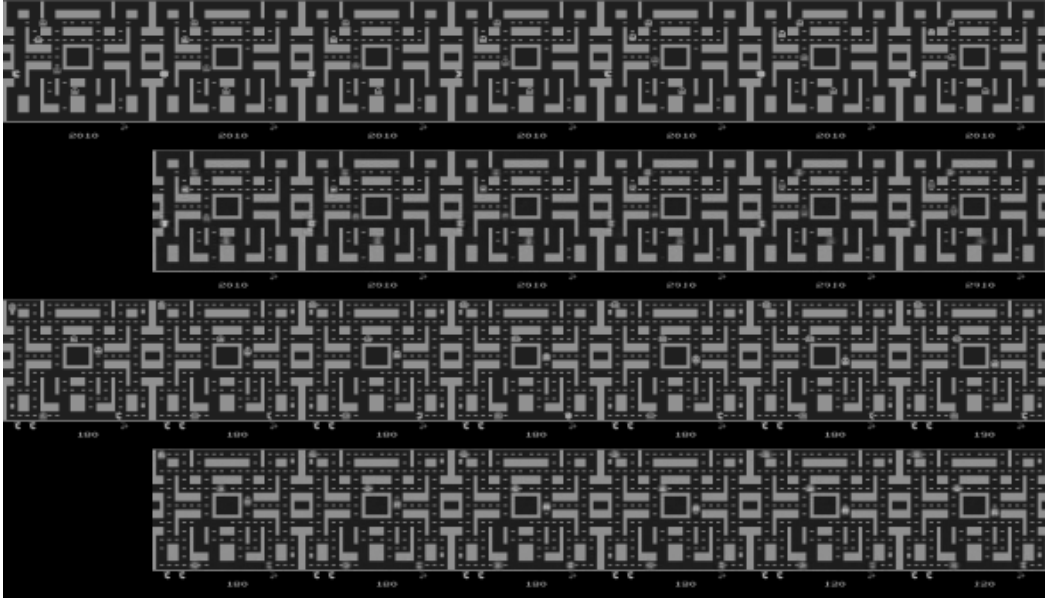


Figure 8: Multi-step prediction result for *Ms_pacman*.

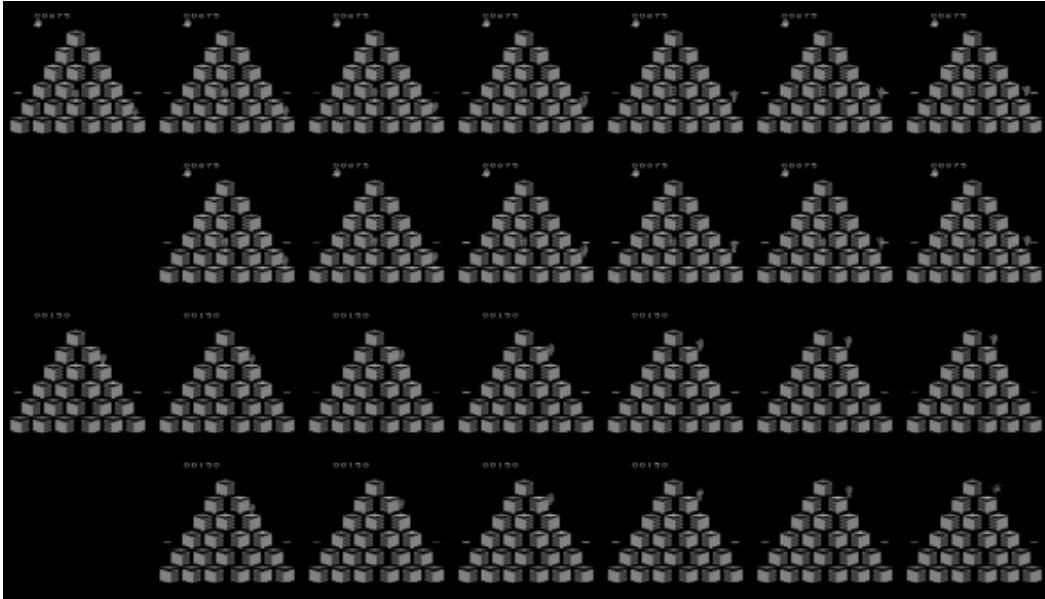


Figure 9: Multi-step prediction result for *Qbert*.

Appendix C.

Result for Hashing over Image Frames

We demonstrate the effect of hashing over image frames in Figure 10. For each domain, we show a set of image frames that are hashed into the same hash code in a row.

Overall, by adopting hashing-based counting approach, we expect that the hashing mechanism could consist of certain degree of generalization ability, so that similar frames could be hashed into the same hash code, while dissimilar frames could be distinguished. To this end, using features derived from autoencoder layer is apparently better than using raw pixels, since the image frames are too distinct at pixel level. However, when using autoencoder features, it is extremely hard to control the degree of generalization achieved by the output of the feature layer. Moreover, the binarization approach via LSH and the additional training phase of autoencoder to match the codes for predicted frames and the real seen frames makes it even harder to ensure that the degree of generalization for the hash code is within an expected level.

From the results shown in Figure 10, we observe the hashing mechanism could identify some significant game-related features. For instance, in *Breakout*, we find the hash code is much more sensitive to the shape of bricks and board positions than the ball position; in *Freeway*, the intensity of cars and the position of the cars matters; in *Frostbite*, the hash codes distinguish well on the layout of platform pattern. However, we also find the current limitation of representing multiple patterns by one code, and the challenge of distinguishing frames based on some desired game-related feature, such as the ball position for *Breakout*, which may fail to be captured by the hashing mechanism without intelligently tune the hashing mechanism based on the desired purpose.

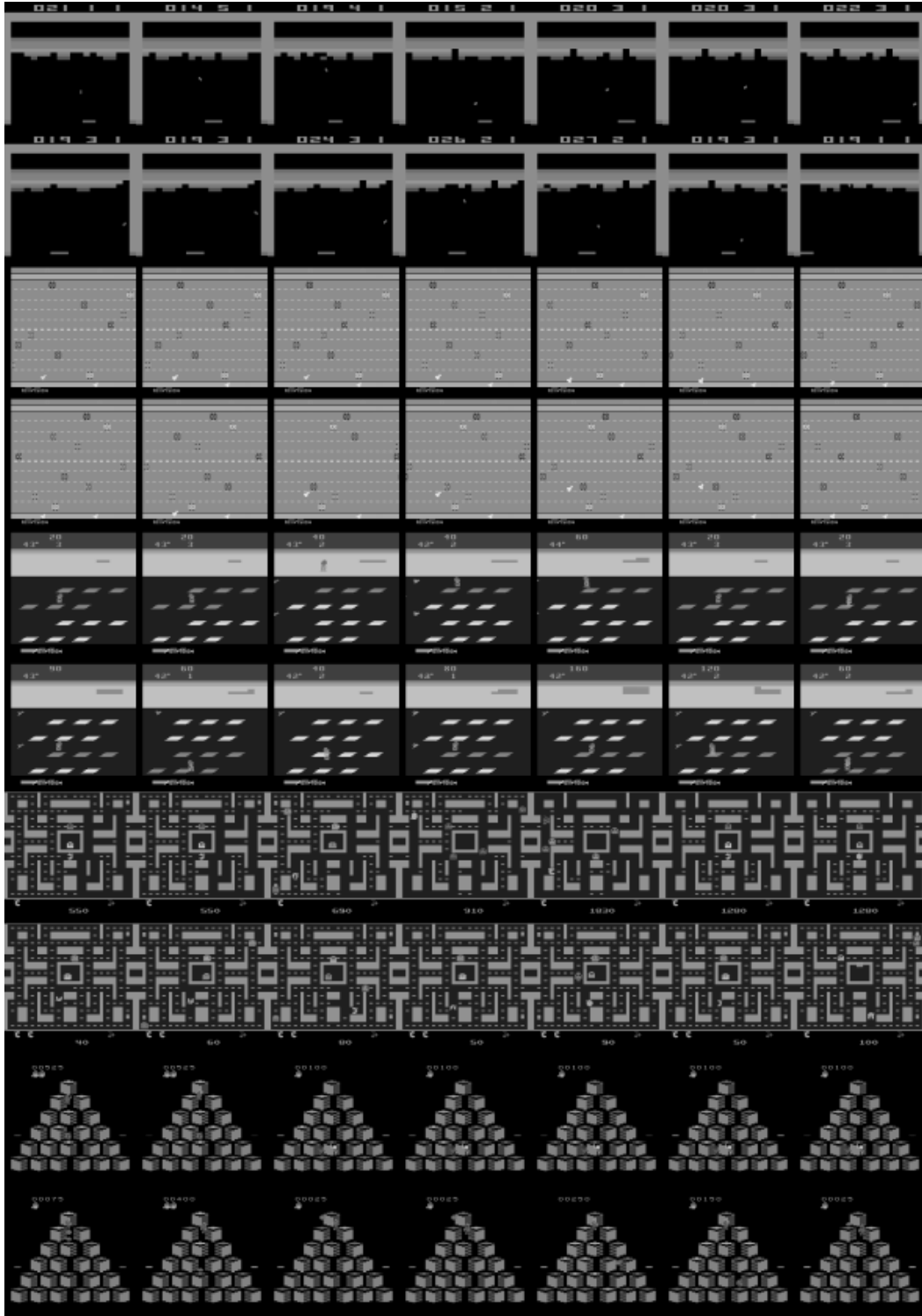


Figure 10: Result for hashing over image frames in each domain. Each row corresponds to the frames that lead to the same hash code in that corresponding game domain.